

ASCA OBSERVATIONS OF PSR 1929+10 AND PSR 0950+08

F. Y.-H. WANG AND J. P. HALPERN

Columbia Astrophysics Laboratory, Columbia University, 550 West 120th Street, New York, NY 10027;
fyw@tommy.phys.columbia.edu; jules@carmen.phys.columbia.edu

Received 1997 March 18; accepted 1997 April 8

ABSTRACT

The *ASCA* X-ray spectra of the old pulsars PSR 1929+10 and PSR 0950+08 are adequately fitted by simple blackbodies. Between 0.5 and 5.0 keV, PSR 1929+10 is best fitted with $T = (5.14 \pm 0.53) \times 10^6$ K and $L = 1.54 \times 10^{30}$ ergs s^{-1} ; PSR 0950+08 has $T = (5.70 \pm 0.63) \times 10^6$ K and $L = 4.67 \times 10^{29}$ ergs s^{-1} . The inferred areas are 2 orders of magnitude smaller than canonical polar cap sizes. There is some evidence for a dearth of photons above 5 keV, which would disfavor alternative power-law models for the spectra. Pulsed emission is detected from PSR 1929+10 with 99.8% significance and pulsed fraction 0.35 ± 0.15 . Marginal evidence of pulsed X-ray emission from PSR 0950+08 is present with 99.0% significance and pulsed fraction 0.34 ± 0.18 . Relativistic ray tracing shows that if the geometry deduced from the polarization of the radio pulse is adopted for the surface thermal emission, a centered dipole cannot reproduce the large pulse modulations observed unless the radius of the neutron star is as large as 18 km. A mechanism of polar cap heating by the impact of relativistic particles is suggested that can produce small areas with $T \sim 5 \times 10^6$ K on old, spun-down pulsars with weak magnetic fields ($B \sim 3 \times 10^{11}$ G).

Subject headings: pulsars: individual (PSR 0950+08, PSR 1929+10) — stars: neutron — X-rays: stars

1. INTRODUCTION

PSR 1929+10 ($\tau = 3.1 \times 10^6$ yr) and PSR 0950+08 ($\tau = 1.7 \times 10^7$ yr) are the oldest of the ordinary (spun-down) pulsars that are well detected in X-rays. A good detection of pulsation was made in the *ROSAT* PSPC observation of PSR 1929+10 (Yancopoulos, Hamilton, & Helfand 1994), but no periodicity was found in the much shorter *ROSAT* observation of PSR 0950+08 (Manning & Willmore 1994). The X-ray spectra of both objects were interpreted as thermal emission from a very small fraction of the surface of the neutron star. The best-fitted blackbody temperatures were $\approx 3 \times 10^6$ K; at this temperature, most photons fall near 1 keV. As the *Advanced Satellite for Cosmology and Astrophysics (ASCA)* has broader response and better energy resolution in this band, it can usefully investigate these two pulsars. Both are faint X-ray sources, and the results gleaned from *ROSAT* are far from conclusive. Therefore, we undertook an independent analysis of archival *ASCA* observations to obtain more information on the X-ray properties of these two pulsars.

2. OBSERVATIONS

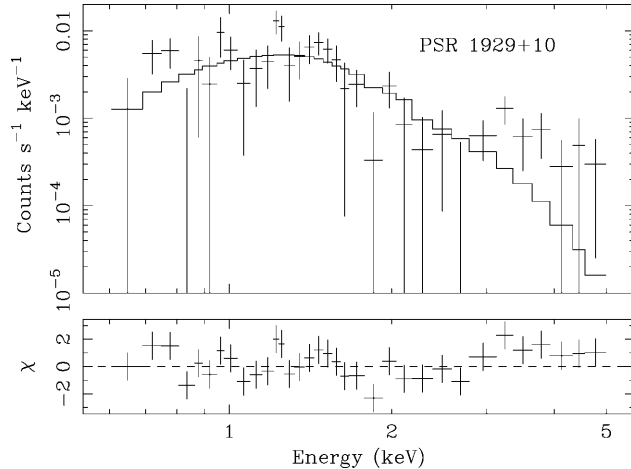
PSR 1929+10 was observed with *ASCA* on 1994 October 17. The source was placed at the standard 1 CCD position in the SIS. After screening the data with standard criteria, a useful exposure duration of 54 ks remained in the SIS. In order to achieve higher time resolution in the GIS, four position bits and two PHA bits were sacrificed, yielding $1' \times 1'$ pixels instead of $15'' \times 15''$ pixels, and 256 spectral channels instead of 1024. The time resolution achieved was 7.8 ms. PSR 0950+08 was observed on 1994 November 29, with exposure duration of 40 ks in the SIS after screening. The pulsar was placed at the center of GIS3, but on SIS0 it was only $1'$ from the edge of the CCD. Full position resolution was retained in this GIS observation, but two PHA bits and five rise time bits were reassigned to timing bits, yielding a time resolution of 3.9 ms.

3. SPECTRAL ANALYSIS

The data were reduced using the FTOOLS/XSELECT software package. Among the four detectors, we found that SIS0 provided the best spectrum. For PSR 1929+10 we used a source extraction radius of $3'$, as is recommended for weak sources. Various trial background regions were tested. Although the spectral shape of the background varies little with off-axis position, its flux varies significantly. Therefore, we chose an annulus surrounding the source to sample a region of similar background intensity. After background subtraction the source count rate in SIS0 is $(7.3 \pm 0.9) \times 10^{-3}$ s^{-1} . Because of the uncertainty of the instrumental response at low energies and the large background rate at high energies, we restrict our spectral fits to the range 0.5–5.0 keV.

The spectrum of PSR 1929+10 (Fig. 1) can be fitted with a single blackbody. The fitted parameters and 68% confidence errors are listed in Table 1. The neutral hydrogen column density is not included as a free parameter, since it is expected to be only $\approx 1 \times 10^{20}$ cm^{-2} for PSR 1929+10 based on its dispersion measure of 3.176 cm^{-3} pc (Taylor, Manchester, & Lyne 1993), and it would not affect the *ASCA* spectrum significantly. The luminosity is calculated for the distance of 250 pc estimated by Yancopoulos et al. (1994), and it corresponds to emitting area $A = 3.2 \times 10^7$ cm^2 .

A power-law model with energy index $\alpha = 0.79 \pm 0.23$ fits PSR 1929+10 almost as well, as indicated in Table 1. A measurement of the spectrum above 5 keV would be crucial in determining which model provides a superior description of the spectrum. Unfortunately, the background dominates above 5 keV, where it can only be estimated that 12 ± 6 net photons are present in the source. It is not certain whether this constitutes a real detection or a systematic error in the background subtraction. The best-fitting blackbody model predicts that there would be essentially zero photons above 5 keV, but extrapolation of the allowed range of power-law fits

FIG. 1.—Blackbody fit to the *ASCA* SIS0 spectrum of PSR 1929+10.

in Table 1 predicts 37–52 photons. This is perhaps weak evidence in favor of the blackbody model.

PSR 0950+08 was observed only 1' from the edge of the CCD in SIS0, so we chose a circle of 2.5 radius, part of which is truncated, as our source region. The background photons were collected at least 3' from the source. The count rate of PSR 0950+08 in SIS0 is $(7.1 \pm 0.8) \times 10^{-3} \text{ s}^{-1}$. The parameters of the blackbody and power-law fits are listed in Table 1. The blackbody fit, shown in Figure 2, is only slightly better than the power law. Once again, the dearth of X-ray photons above 5 keV provides some additional support for the blackbody model. There are only 13 ± 6 source photons above 5 keV, while the power-law extrapolation predicts 42–58, and the blackbody less than 2.

Although GIS3 is not as sensitive for spectral analysis, we used it for PSR 0950+08 to check the overall flux because the source was very close to the edge of the SIS0 CCD. The spectrum in GIS3 was fitted with a blackbody, yielding a temperature not significantly different from the SIS0 value. However, the GIS3 flux was 29% higher than that of SIS0, which we interpret as that fraction of photons falling outside the boundary of the SIS0 CCD. The fluxes in Tables 1 and 2 were adjusted accordingly to match the GIS3 flux. The lumi-

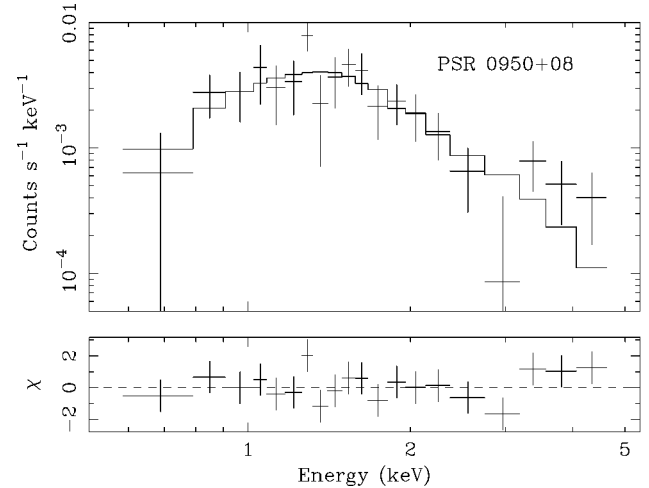
TABLE 1
SINGLE-COMPONENT FITS TO *ASCA* SPECTRA

| Parameter | PSR 1929+10 | PSR 0950+08 |
|---|--|--|
| Blackbody Fits | | |
| T (K)..... | $(5.14 \pm 0.53) \times 10^6$ | $(5.70 \pm 0.63) \times 10^6$ |
| χ^2_ν | 1.31/31 | 0.84/18 |
| F (ergs $\text{cm}^{-2} \text{s}^{-1}$) ^a | 1.71×10^{-13} | 1.87×10^{-13} |
| L (ergs s^{-1}) ^a | $1.28 \times 10^{30} (d/250 \text{ pc})^2$ | $3.50 \times 10^{29} (d/125 \text{ pc})^2$ |
| A (cm^2)..... | $3.2 \times 10^7 (d/250 \text{ pc})^2$ | $5.8 \times 10^6 (d/125 \text{ pc})^2$ |
| Power-Law Fits | | |
| α | 0.79 ± 0.23 | 0.40 ± 0.22 |
| C^b | $(6.1 \pm 1.6) \times 10^{-5}$ | $(5.2 \pm 1.4 \times 10^{-5})$ |
| χ^2_ν | 1.35/31 | 1.01/18 |
| F (ergs $\text{cm}^{-2} \text{s}^{-1}$) ^c | 2.50×10^{-13} | 2.77×10^{-13} |
| L (ergs s^{-1}) ^c | $1.87 \times 10^{30} (d/250 \text{ pc})^2$ | $5.18 \times 10^{29} (d/125 \text{ pc})^2$ |

^a Bolometric.

^b Normalization ($\text{keV cm}^{-2} \text{s}^{-1} \text{keV}^{-1}$) at 1 keV.

^c In the range 0.5–5.0 keV.

FIG. 2.—Blackbody fit to the *ASCA* SIS0 spectrum of PSR 0950+08.

nosity of PSR 0950+08 is calculated for a distance of 125 pc, according to the parallax measurement of Gwinn et al. (1986); it implies emitting area $A = 5.8 \times 10^6 \text{ cm}^2$.

For both pulsars, we are unable to discriminate conclusively between thermal and nonthermal spectra. While a blackbody is a better fit overall, the inferred emitting areas are surprising small. Furthermore, the possible excess in counts above 5 keV could represent an additional, nonthermal component. Alternatively, such hard photons could have their origin in the atmosphere of a hot polar cap whose opacity decreases at higher energy (Pavlov et al. 1994; Zavlin et al. 1995a). An overall hardening of the spectrum due to nongray atmospheric opacity might imply that the effective temperature is smaller, and the emitting area larger, than the blackbody fitted values listed in Table 1.

4. TIMING ANALYSIS

Timing analysis is possible only with the GIS instruments. The photon arrival times are converted to TDB with the program “timeconv” in FTOOLS. For PSR 1929+10 we extracted the photons from a circle of radius 2.5 in both GIS2 and GIS3. The total counts in the range 0.5–5.0 keV number 747, of which 413 are estimated to be background. In the observation of PSR 0950+08, the signal-to-background ratio

TABLE 2
PULSAR DATA^a

| Parameter | PSR 1929+10 | PSR 0950+08 |
|--|--|--|
| α (J2000)..... | 19 ^h 32 ^m 13 ^s .914 | 9 ^h 53 ^m 9 ^s .307 |
| δ (J2000)..... | +10 ^o 59'32".33 | +7 ^o 55'35".93 |
| T_0 (MJD) ^b | 49668.0 | 49430.0 |
| f (Hz)..... | 4.4146611894452 | 3.9515504263058 |
| \dot{f} (Hz s^{-1})..... | -2.25218×10^{-14} | -3.59533×10^{-15} |
| \ddot{f} (Hz s^{-2})..... | 2.40×10^{-24} | 1.43×10^{-25} |
| B (G)..... | 5.1×10^{11} | 2.5×10^{11} |
| τ (yr)..... | 3.1×10^6 | 1.7×10^7 |
| \dot{E} (ergs s^{-1}).... | 3.9×10^{33} | 5.6×10^{32} |

^a Taylor, Manchester, & Lyne 1993.

^b Barycentric (TDB) epoch and phase 0 in Figs. 3 and 4.

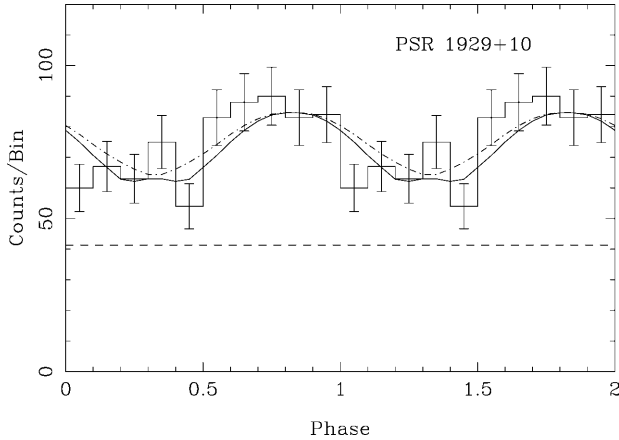


FIG. 3.—Pulse profile of PSR 1929+10 in the 0.5–5.0 keV band; the dashed line indicates the background level, and the dot-dashed line represents the simulated curve with $M = 1.4 M_{\odot}$, $R = 10$ km, one polar cap, and Phillips's geometry, $\alpha = 31^{\circ}$ and $\xi = 51^{\circ}$. The solid line is a fit using two polar caps and $R = 18$ km.

in GIS2 was evidently very poor. Therefore, we use only GIS3, taking the photons from a circle of radius $3'$. Here, the total counts in the range 0.5–5.0 keV number 507, of which 283 are background.

The collected photons are folded according to the radio ephemeris (Taylor et al. 1993); the light curves appear in Figures 3 and 4. The significance of the detected modulation was assessed using the Z_n^2 test (Buccheri et al. 1983). For PSR 1929+10, $Z_1^2 = 12.3$, whereas for PSR 0950+09, $Z_1^2 = 9.2$, corresponding to chance probabilities 0.0021 and 0.010, respectively. The pulsed fraction, defined as the fraction of counts above the minimum in the light curve, is estimated to be 0.35 ± 0.15 for PSR 1929+10, and 0.34 ± 0.18 for PSR 0950+09.

Both light curves are characterized by a single broad maximum. Structure of this kind might be produced by one or two heated spots on the surface of a neutron star subject to gravitational bending of light. We employed a relativistic ray-tracing code to simulate light curves (see Chen & Shaham

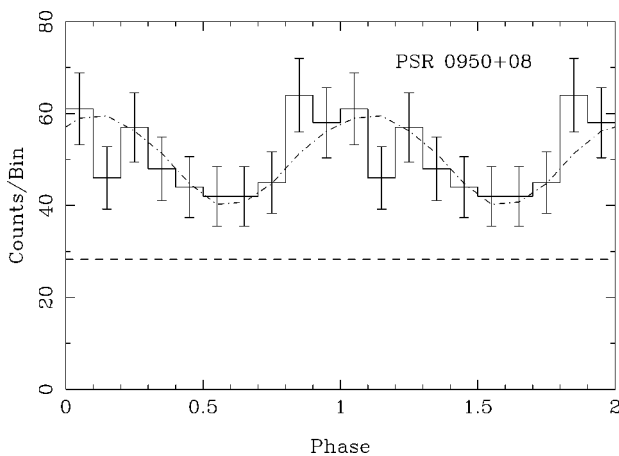


FIG. 4.—Pulse profile of PSR 0950+08 in the 0.5–5.0 keV band; the dashed line indicates the background level, and the dot-dashed line represents the simulated curve with $M = 1.4 M_{\odot}$, $R = 10$ km, one polar cap, and the hypothetical geometry, $\alpha = \xi = 45^{\circ}$.

1989), assuming isotropic thermal emission on the surface. The pulsed fraction depends strongly on the angle between the spin and magnetic axes α , and the parameter $(1+z) = (1 - 2GM/Rc^2)^{-1/2}$, but insensitively on the size of the polar cap. The canonical pulsar model, with a dipole centered on the neutron star, generates weak modulation, typically less than 10%, unless M/R is small. One heated polar cap, or sunspot-like polar caps less than about 10° apart, produces a larger pulsed fraction.

Lyne & Manchester (1988) described PSR 1929+10 and PSR 0950+08 as nearly aligned rotators based on the shape and polarization of their radio pulses. Such a configuration fails to generate the X-ray light curves that we observed. Phillips (1990) determined the geometry of PSR 1929+10 with more sensitive data; he found the angle between the spin and magnetic axes, $\alpha = 31^{\circ} \pm 2^{\circ}$, and the angle between the spin axis and the line of sight, $\xi = 51^{\circ} \pm 2^{\circ}$. Adopting Phillips's geometry, with $M = 1.4 M_{\odot}$, $R = 10$ km, and a single polar cap, we simulated the curve plotted in Figure 3. The simulated curve fits our data reasonably well: $\chi_r^2 = 1.17$ with 9 degrees of freedom. But with two polar caps 180° apart, we cannot produce a modulation as large as that observed, because gravitational bending fills in the minimum of the light curve with rays from the opposite polar cap. This difficulty implies that the centered dipole with two polar caps might not describe the magnetic structure near the surface of a neutron star. Alternatively, the modulation can be increased to the observed value of 30% by increasing the radius to $R = 18$ km, which provides a fit that is nearly as good as the single polar cap with $R = 10$ km (see Fig. 3).

For PSR 0950+08 we simulated several light curves based on hypothetical polar cap geometries. With one polar cap, $M = 1.4 M_{\odot}$, and $R = 10$ km, the angle α must be $\approx 45^{\circ}$ for the pulsed fraction to match our light curve. The simulated light curve in Figure 4 has $\alpha = \xi = 45^{\circ}$. According to this model, with one polar cap (or two polar caps that are closed to each other), we estimate $\alpha \approx \xi \approx 45^{\circ} \pm 10^{\circ}$.

Models of pulsar light curves employing isotropically emitting hot spots in the centered dipole geometry have been explored by Zavlin, Shibano, & Pavlov (1995b), while including those same atmospheric effects that modify the blackbody spectrum. They showed that anisotropic opacity in a strong magnetic field narrows the emergent X-ray beam, assuming that the magnetic field is normal to the surface of the star at the heated polar cap, because X-rays escape preferentially along the magnetic field direction. Even so, the light curves that they simulated for PSR 1929+10 using $M \geq 1.4 M_{\odot}$ and a centered dipole fail to reproduce the broad, sinusoidal modulation that is observed. Instead, they produce a narrow main peak and a pulsed fraction that is smaller than that observed. Their light curves for emission from just one hot spot resemble our data more closely. Therefore, we consider that the analysis of Zavlin et al. (1995b), under more sophisticated assumptions about the neutron star atmosphere, supports our impression that an off-center magnetic field geometry is required.

5. DISCUSSION AND CONCLUSIONS

PSR 1929+10 and PSR 0950+08 are old pulsars, with characteristic age $\tau = 3.1 \times 10^6$ yr and 1.7×10^7 yr, respectively. Cooling models (Nomoto & Tsuruta 1987; Lattimer et

al. 1991; Page & Applegate 1992) predict the surface temperature of a neutron star to be $\leq 10^5$ K at this age. Therefore, in modeling the *ASCA* detected X-rays as thermal emission with $T \approx 5 \times 10^6$ K, one assumes that there is some reheating mechanism. One candidate for this mechanism is polar cap heating by the impact of charged particles accelerated in the magnetosphere (Halpern & Ruderman 1993). Perhaps the greatest obstacle to such an interpretation is the tiny sizes implied for the polar caps, which are 2 orders of magnitude smaller than the canonical open field line value $A_0 = 6.6 \times 10^6 P^{-1} \text{ cm}^2$, in which P is the period in seconds. However, A_0 applies to the ideal case of a point magnetic dipole located at the center of the neutron star. This may be a good approximation for the outer magnetosphere, but it is probably inadequate to describe the complicated distribution of the magnetic field on the surface of a neutron star. Both pulsars have a weak surface dipole magnetic field ($B \approx 3 \times 10^{11}$ G), which might be evidence for evolution of the magnetic field (Ruderman 1991). The stellar magnetic flux may emanate from strongly magnetized platelets on the crust. While the average surface dipole field is diminished, the rather uniform platelet field B_p remains frozen at its initial value, $B_p \sim 3 \times 10^{12}$ G. Hence, the surface flux becomes squeezed into smaller areas (see Chen & Ruderman 1993a), $A_{pc} \sim (\langle B \rangle / B_p) A_0 \sim 0.1 A_0$. An additional factor that could further reduce the size of the heated polar cap in these pulsars is their relatively small spin-down power, $\dot{E} \sim 10^{33} \text{ ergs s}^{-1}$. They are not expected to be able to power an outer magnetosphere accelerator and its associated strong pulsed γ -ray emission (Chen & Ruderman 1993b). Without an outer magnetosphere accelerator as a supplier of copious charged particles, the full Goldreich-Julian current may not be achieved, and only a small part of the polar cap may be activated. For this reason the X-rays might seem to

be emitted from a small area. The temperature of the heated part of the polar cap is estimated to be

$$T \sim \left(E_f \frac{\Omega B_p}{2\pi e \sigma} \right)^{1/4} \sim 5 \times 10^6 \text{ K} \quad (1)$$

(Ruderman & Sutherland 1975), in which $E_f \sim 1$ erg is the energy acquired by charged particles in the polar cap accelerator, and $\Omega B_p / 2\pi e$ is the Goldreich-Julian current density. This is consistent with our best-fitted temperatures.

In conclusion, we have measured X-ray fluxes and pulse shapes of PSR 1929+10 and PSR 0950+08 with *ASCA* that are consistent with *ROSAT* results (Yancopoulos et al. 1994; Manning & Willmore 1994), although the *ASCA* measured temperatures are higher. Although the simplest adequate spectral model of both of these is surface blackbody emission presumed to be coming from heated polar caps, difficulties are encountered in explaining the tiny emitting areas inferred and the large pulse modulation observed. Modifications to the spectrum and beam pattern resulting from an off-center dipole geometry and anisotropic opacity, in addition to the hypothesized reduction in polar cap area and backflow current discussed above, are likely to play important roles in explaining these observations. Much more data are needed to better characterize the X-ray spectra and pulse profiles of these old pulsars and to quantify the magnitude of these various theoretical effects.

We thank M. Ruderman and K. Chen for enlightening discussions, and K. Leighly and D. J. Helfand for suggestions about *ASCA* data analysis. This work was supported by NASA grants NAG 5-2524 and NAG 5-3229. This Letter is contribution 631 of the Columbia Astrophysics Laboratory.

REFERENCES

- Buccheri, R., et al. 1983, *A&A*, 128, 245
 Chen, K., & Ruderman, M. 1993a, *ApJ*, 408, 179
 ———. 1993b, *ApJ*, 402, 264
 Chen, K., & Shaham, J. 1989, *ApJ*, 339, 279
 Gwinn, C. R., Taylor, J. H., Weisberg, J. M., & Rawley, L. A. 1986, *AJ*, 91, 338
 Halpern, J. P., & Ruderman, M. 1993, *ApJ*, 415, 286
 Lattimer, J. M., Pethick, C., Prakash, C. J., & Haensel, P. 1991, *Phys. Rev. Lett.*, 49, 1373
 Lyne, A. G., & Manchester, R. N. 1988, *MNRAS*, 234, 477
 Manning, R. A., & Willmore, A. P. 1994, *MNRAS*, 266, 635
 Nomoto, K., & Tsuruta, S. 1987, *ApJ*, 312, 711
 Page, D., & Applegate, J. H. 1992, *ApJ*, 394, L17
 Pavlov, G. G., Shibano, Yu. A., Ventura, J., & Zavlin, V. E. 1994, *A&A*, 289, 837
 Phillips, J. A. 1990, *ApJ*, 361, L57
 Ruderman, M. 1991, *ApJ*, 382, 587
 Ruderman, M. A., & Sutherland, P. G. 1975, *ApJ*, 196, 51
 Taylor, J. H., Manchester, R. N., & Lyne, A. G. 1993, *ApJS*, 88, 529 (revisions at Princeton Pulsar Database, file://pulsar.princeton.edu/gro/)
 Yancopoulos, S., Hamilton, T. T., & Helfand, D. J. 1994, *ApJ*, 429, 832
 Zavlin, V. E., Pavlov, G. G., Shibano, Yu. A., & Ventura, J. 1995a, *A&A*, 297, 441
 Zavlin, V. E., Shibano, Yu. A., & Pavlov, G. G. 1995b, *AZh Pis'ma*, 21, 168